Decoupled Control of an Active Magnetic Bearing System for a High Gyroscopic Rotor

Markus Hutterer, Matthias Hofer and Manfred Schrödl
Vienna University of Technology
Institute of Energy Systems and Electrical Drives, Austria, 1040 Vienna, Gusshausstrae 25-27
Email:markus.hutterer@tuwien.ac.at

***Abstract*—Control design for coupled MIMO-Systems (Multiple Input and Multiple Output) like a 5-DOF (degree of freedom) AMB (active magnetic bearing) system needs a high knowledge in control theory. This paper describes a model based approach for decoupled control design. To decouple the system an input and an output transformation is used and all control parts are developed in the so called center of gravity (COG) coordinate system. One of the main problems is the stabilization of the rotor for a high speed range. This problem is solved by a parameter variant feedback path, which transforms the linear parameter variant system in a linear parameter invariant system. This feedback path requires the angular velocity and the velocities of the degrees of freedom for calculation. The angular velocity can be used from the motor controller. For the other velocities a Kalman observer is used. This Kalman observer is developed only in the center of gravity coordinates, because in this coordinate system the observer needs less computing power. The stability and robustness of the closed loop system is verified by simulations and experimental results.**

***Keywords*—AMB System, Gyroscopic effect, Model based control, Flexible rotor.**

I. INTRODUCTION

Magnetic bearings are used in many industrial applications, because of their big advantages compared to other bearing types. Advantages are the almost frictionless and wearless operation. They do not need lubricants and are maintenance free. For a stable levitation the magnetic bearing force is provided dependent on the position of the rotor which is measured by a position sensor ([1],[2]). In the last years also a few sensorless control strategies were developed, like the INFORM method which is described in [3] and [4]. A 5-DOF AMB system is described with a coupled parameter variant differential equation system, where it is generally not easy to find a feedback path with a good performance. The most straightforward method is to feed every sensor back to the actuator of the same degree of freedom. This strategy is called decentralized control method [5]. The advantage of this method is that the proportional part of the controller could be physically interpreted as a spring and the differential part as a damper. The drawback is that the input and output matrix of the state space description causes non diagonal terms. As a consequence the tilting and translation modes cannot be treated independent from each other. Tilting means the rotation movement with the angles (α and β) and translation represents movements along the coordinates (x_s and y_s). To eliminate this problem a special central controller is used which cancels all non diagonal matrices. Because the stiffness matrix is constant, the compensation term of this matrix gets constant too and can be calculated offline. In contrast to this cancelation the gyroscopic matrix is depended on the angular velocity [6], so the matrix has to be calculated in every sample period. To control the tilting and translation modes independently input and output transformations of the controller are introduced.

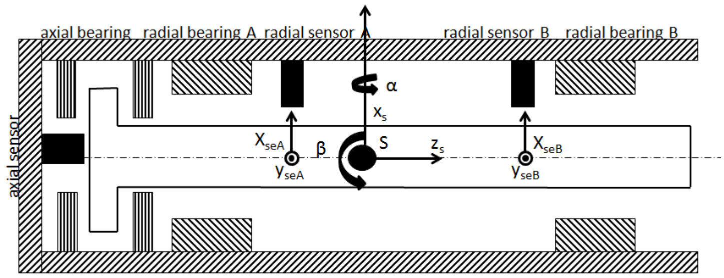

Fig. 1. 5-DOF AMB System

The paper is organized as follows. In section II a illustration of a 5-DOF AMB system is shown and the system equation are explained. Section III shows the control structure and explains the main development steps for designing a controller of an AMB system with a high gyroscopic rotor. The focus of section III is the development of the compensation of the gyroscopic effect. Section IV proves the stability and the performance of the system using simulation results. Experimental results carried on a laboratory AMB system are reported in section V. Finally Section VI summarizes the conclusions of the main developments of this paper.

II. 5-DOF AMB SYSTEM

A 5-DOF AMB system consists of two radial bearings and one axial bearing as shown in Fig.1. To achieve a stable levitation every DOF requires a position sensor. In this paper the radial and axial bearings are separated for control design. This is possible under a few assumption which are described in [7]. The mathematical model of a rigid rotor which is supported by a 5-DOF AMB system used COG coordinates is:

$$\begin{aligned}\mathbf{M}\ddot{\mathbf{x}} + \mathbf{G}(\omega)\dot{\mathbf{x}} + \mathbf{B}\mathbf{K}_S\mathbf{B}^T\mathbf{x} &= \mathbf{B}\mathbf{K}_i\mathbf{i} \\ \mathbf{y} &= \mathbf{C}\mathbf{x}\end{aligned} \tag{1}$$

with

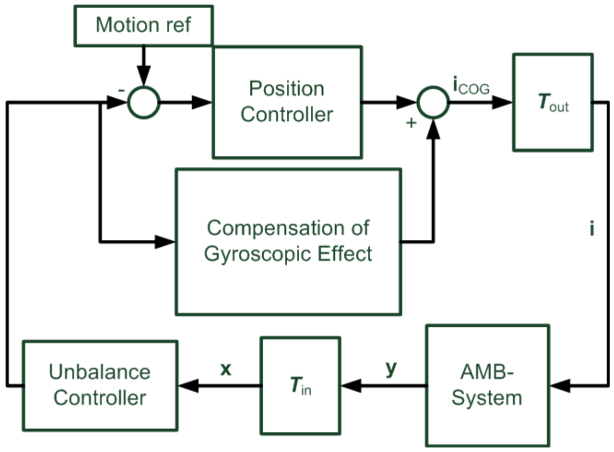

Fig. 2. Control structure of the AMB-System

$$\mathbf{M}=\begin{bmatrix} I_x & 0 & 0 & 0\\ 0 & m & 0 & 0\\ 0 & 0 & I_x & 0\\ 0 & 0 & 0 & m \end{bmatrix} \quad \mathbf{G}=\begin{bmatrix} 0 & 0 & I_p\omega & 0\\ 0 & 0 & 0 & 0\\ -I_p\omega & 0 & 0 & 0\\ 0 & 0 & 0 & 0 \end{bmatrix}$$

$$\mathbf{K}_S=\begin{bmatrix} k_{sa} & 0 & 0 & 0\\ 0 & k_{sb} & 0 & 0\\ 0 & 0 & k_{sa} & 0\\ 0 & 0 & 0 & k_{sb} \end{bmatrix} \quad \mathbf{B}=\begin{bmatrix} a & b & 0 & 0\\ 1 & 1 & 0 & 0\\ 0 & 0 & a & b\\ 0 & 0 & 1 & 1 \end{bmatrix}$$

$$\mathbf{C}=\begin{bmatrix} c & 1 & 0 & 0\\ d & 1 & 0 & 0\\ 0 & 0 & c & 1\\ 0 & 0 & d & 1 \end{bmatrix} \quad \mathbf{y}=\begin{bmatrix} x_{seA}\\ x_{seB}\\ y_{seA}\\ y_{seB} \end{bmatrix}$$

$$\mathbf{K}_i=\begin{bmatrix} k_{ia} & 0 & 0 & 0\\ 0 & k_{ib} & 0 & 0\\ 0 & 0 & k_{ia} & 0\\ 0 & 0 & 0 & k_{ib} \end{bmatrix} \quad \mathbf{i}=\begin{bmatrix} i_{xA}\\ i_{xB}\\ i_{yA}\\ i_{yB} \end{bmatrix} \quad \mathbf{x}=\begin{bmatrix} \beta\\ x_s\\ \alpha\\ y_s \end{bmatrix}$$

Where k_{ia} and k_{ib} are the linearized force current factors, k_{sa} and k_{sb} are the linearized force displacement factors, a and b are the distances from the magnetic bearings to the center of gravity, c and d are the distances from the position sensors to the center of gravity, m is the mass of the rotor, I_x is the equatorial moment of inertia, $\mathbf{G}(\omega)$ is the parameter variant gyroscopic matrix, I_p is the polar moment of inertia, ω is the angular velocity, and $\mathbf{i}$ is the current vector from the current controller. Usually the equation of this system is more complicated and nonlinear, but with k_s and k_i the electromagnetic force is linearized. The index S means that the coordinates are in the center of gravity and seA or seB that the axes are at the position sensors.

III. DESIGN OF THE CONTROLLER

In this section the whole control structure of the AMB is explained. Fig. 2 shows a schematic illustration of the implemented control structure. The unbalance controller is a generalized Notch filter, which is explained in [10]. The other blocks of the control structure are explained in the following sub chapters.

A. Input and output Transformation

To effect the tilting and the translation mode independent from each other a transformation from the sensor coordinates to the so called center of gravity (COG) coordinate system of the rigid body model is necessary. The following transformation are the derived under the assumptions that the matrices $\mathbf{C}$ and $\mathbf{BK}_i$ are invertible. Equation (1) shows that $\mathbf{T}_{in}$ can be calculated with:

$$\mathbf{T}_{in}=\mathbf{C}^{-1} \tag{2}$$

With this input transformation the whole control structure has to be developed in the COG coordinate system. But it has to be considered that the output value of the controller is also given in the COG coordinate system. To transform the output values back, $\mathbf{T}_{out}$ is used. From equation (1) can be seen that a possibility for $\mathbf{T}_{out}$ is:

$$\mathbf{T}_{out}=(\mathbf{BK}_i)^{-1} \tag{3}$$

Now the rigid body model with both transformations has the following form:

$$\mathbf{M}\ddot{\mathbf{x}}+\mathbf{G}(\omega)\dot{\mathbf{x}}+\mathbf{BK}_S\mathbf{B}^T\mathbf{x}=\mathbf{BK}_i\,(\mathbf{BK}_i)^{-1}\,\mathbf{i} \tag{4}$$

$$\mathbf{M}\ddot{\mathbf{x}}+\mathbf{G}(\omega)\dot{\mathbf{x}}+\mathbf{BK}_S\mathbf{B}^T\mathbf{x}=\mathbf{i} \tag{5}$$

Now the tilting and translation modes can be influenced nearly independent from each other. A big advantage of this method is that the gyroscopic effect only are present in the tilting modes. But one coupling between both modes is still present, because the Matrix $\mathbf{BK}_S\mathbf{B}^T$ is not diagonal. So an additional feedback term $\mathbf{K}_{scomp}$ is needed. Now the control structure can be described with:

$$\mathbf{i}=\mathbf{T}_{out}\,(\mathbf{v}+\mathbf{K}_{scomp}\mathbf{T}_{in}\mathbf{y}) \tag{6}$$

with

$$\mathbf{K}_{scomp}=\mathbf{BK}_S\mathbf{B}^T \tag{7}$$

Where $\mathbf{v}$ is the new input. In the resulting system the tilting movement becomes independent from the translation movements for this new input $\mathbf{v}$.

$$\mathbf{M}\ddot{\mathbf{x}}+\mathbf{G}(\omega)=\mathbf{v} \tag{8}$$

But the natural frequencies of the tilting and translation movements are not constant for increasing speeds, because of the gyroscopic effect. For rotors with a high gyroscopic effect, this could lead to instability for some angular velocities. Fig. 3 shows the stability of the system for the predefined speed range. The natural frequencies of the translation movement at about 65Hz is speed independent and has also a constant damping ratio. Compared to this it is much more difficult to find a stable solution for the tilting movement, because the gyroscopic effect splits the modes beginning at 40Hz at 0rpm up to a forward and a backward whirl. Without consideration this effect the controller gets unstable for high frequencies. This can be seen by the negative damping according to Fig. 3. The virtual modes are no mechanical resonances, they are caused by additional eigenvalues of the control structure.

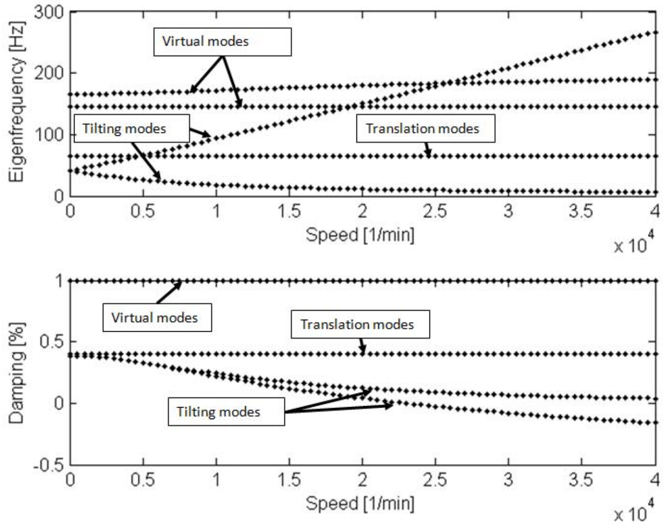

Fig. 3. Stability analysis of the complete speed range

B. Considering the gyroscopic effect

Because the system has a parameter variant term additional work has be done to use LTI control theory. To solve this problem the parameter variant term should be decreased. If the parameter variant part is eliminated or very low for a new input, LTI control theory can be used. If the control law

$$\mathbf{i} = \mathbf{T}_{out}\left(\mathbf{v} + \mathbf{K}_{scomp}\mathbf{T}_{in}\mathbf{y}\right) + \mathbf{G}\dot{\mathbf{x}} \tag{9}$$

is used, The resulting system is a decoupled parameter invariant MIMO system.

$$\mathbf{M}\ddot{\mathbf{x}} = \mathbf{v} \tag{10}$$

with

$$\mathbf{v} = -\mathbf{T}_{con}\mathbf{T}_{in}\mathbf{y} \tag{11}$$

where $\mathbf{T}_{con}$ is the transfer matrix of the position controllers.

In [6] is suggested that a complete elimination of the gyroscopic effect is not very robust against dead times, and therefore a factor C_{att} is introduced.

$$\mathbf{M}\ddot{\mathbf{x}} + \mathbf{G}\left(\omega\right)\left(1 - C_{att}\right)\dot{\mathbf{x}} = \mathbf{v} \tag{12}$$

From equation (12) can be seen that the values of the angular velocities and the velocity information of the COG coordinates are needed. It is possible to use the angular velocity of the motor controller. To estimate the velocities in the COG coordinate system, Kalman observers are used.

C. Kalman observer

If the states of the system are not measurable or the use of sensors are uneconomic, it is possible to use a state observer instead. For MIMO systems it is difficult to find an acceptable observer with the pole placement method. A powerful solution for such a system is a Kalman observer, which minimizes the variance of the estimation error like it was describes in [11]. Generally an extended Kalman filter is used for parameter variant systems. But in this case three different LTI Kalman observers are used for different speed ranges (Table I). The

TABLE I. SPEED RANGES OF THE KALMAN OBSERVERS

	Kalman filter 1	**Kalman filter 2**	**Kalman filter 3**
Speed area	0-15.000rpm	15.000-30.000rpm	30.000-40.000rpm
Design speed	0rpm	20.000rpm	36.000rpm

LTI Kalman observer are used, because they can be calculated much faster than the extended Kalman filter. For filter design the system equation (1) has to be transformed in a discrete state space description

$$\begin{aligned}\mathbf{x}_{k+1} &= \mathbf{\Phi}\mathbf{x}_k + \mathbf{\Gamma}\mathbf{v}_k \\ \mathbf{y} &= \mathbf{C}\mathbf{x}_k\end{aligned} \tag{13}$$

with the states $\mathbf{x}_k$, the output vector $\mathbf{y}_k$, the time discrete dynamic matrix $\mathbf{\Phi}$ and the discrete input matrix $\mathbf{\Gamma}$. A linear Kalman observer for the system (13) has the following form:

$$\hat{\mathbf{x}}_{k+1} = \mathbf{\Phi}\hat{\mathbf{x}}_k + \mathbf{\Gamma}\mathbf{v}_k + \mathbf{K}\left(\mathbf{y}_k - \mathbf{C}\hat{\mathbf{x}}_k\right) \tag{14}$$

The matrix $\mathbf{K}$ is called the Kalman feedback matrix. The theory of developing the matrix $\mathbf{K}$ of a Kalman observer for such a system is shown in [8]. The matrix $\mathbf{K}$ is normally time variant, but in this paper only the stationary solution is used. After computing the feedback matrix, equation (14) is transformed in a representation, where only one matrix multiplication is necessary:

$$\hat{\mathbf{x}}_{kal+1} = \mathbf{A}_{kal}\hat{\mathbf{x}}_{kal} \tag{15}$$

with

$$\hat{\mathbf{x}}_{kal} = \left[\mathbf{y}, \mathbf{i}, \hat{\mathbf{x}}\right]^T \tag{16}$$

Thus, a simplified implementation in the AMB digital controller is achieved. To reduce the computing time of the Kalman observer the zero entries of the Matrix can be increased. In this form $\mathbf{A}_{kal}$ is a 8-by-16 matrix and the controller has to make 128 multiplication for every new state vector. But for the compensation of the gyroscopic effect only the states $\dot{\alpha}$ and $\dot{\beta}$ are needed. If the output and input vector is transformed in the COG coordinate system from the previous subsections, the zero entries of the Kalman filter increase because the tilting and translation modes are decoupled with this input and output coordinates. Because of the independence of both movements a split up of the Kalman observer in a tilting and a translation part is possible. As stated before only the tilting velocities are necessary in this work. This tilting Kalman observer is able to be calculated with a 4-by-8 matrix. Fig. 4 shows the improvement of the Kalman observer graphically. One might expect that the x and y plane are able to split up too, but this is only possible for standstill. The reason is, that the gyroscopic effect would couple both planes. Now the states are able to be estimates with the matrix multiplication

$$\hat{\mathbf{x}}_{tkal+1} = \mathbf{A}_{tkal}\hat{\mathbf{x}}_{tkal} \tag{17}$$

with

$$\hat{\mathbf{x}}_{tkal} = \left[\beta, \alpha, i_\beta, i_\alpha, \hat{\beta}, \hat{\alpha}, \hat{\dot{\beta}}, \hat{\dot{\alpha}}\right]^T \tag{18}$$

This sub chapter shows that it is possible to increase the computing power of a Kalman observer by a factor of 4 with a simple coordinate transformation.

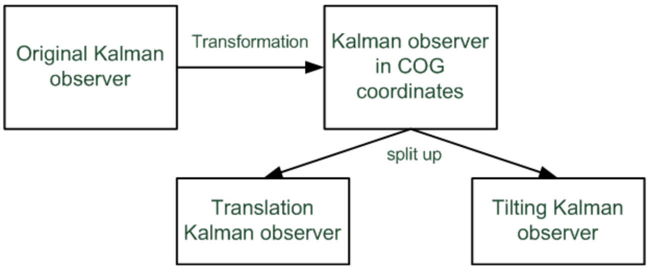

Fig. 4. Improvement steps of the Kalman observer

D. Position Controller

If the compensation of the gyroscopic effect from the previous chapter is used, the system is nearly linear and parameter invariant. For such a system it is possible to find a stable solution in the s-domain. Fig. 5 shows the structure of the position controller. The control structure consists of three parts for every degree of freedom which are implemented as second order IIR filters. Because the first bending mode of the rotor is at about $860Hz$, the control structure is split up in two tasks:

- Stabilize the rigid body modes
- Stabilize the bending modes

For the stabilization of the rigid body modes a PIDT1 controller is used. The PID part is tuned, that the rigid body modes are in the range of 60Hz. To have a separating margin between the two tasks, the T1 part turns off the differentiator at 180Hz. The second order low pass filter in combination with a Lead Lag filter fullfills the task to stabilize the first bending modes and the bending modes for high frequencies. Fig. 6 shows the pole areas where the controller provides stability. The rigid body modes are in the stable area, because of the phase lead from the differentiator. After the differentiator is switched off, the phase of the controller moves in the unstable region, because of the sampling process. The second order lowpass filter shifts the phase from this unstable region in the stable at high frequencies region. Because this phase shift is not fast enough to stabilize the first bending modes, a Lead Lag filter is used to drop the phase locally in the range of the first bending modes. Fig. 7 shows the simulated transfer function of the position controller for the tilting movement. It can be seen that the only range where the controller destabilizes the system is between 210 and 500Hz. This method to stabilize the system for high frequencies could only be used, if the first bending mode has enough separation margin to the rigid body modes. Otherwise additional work has be done to get a stable levitating rotor.

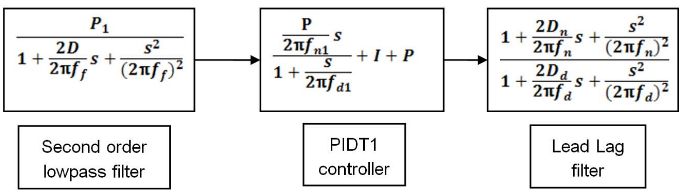

Fig. 5. Control structure of the position controller

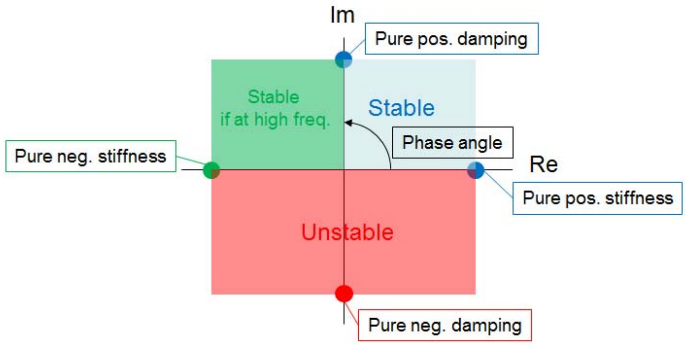

Fig. 6. Stability requirements on the controller [9]

IV. Simulation Results

For the simulation, the rigid body model from section 2 is used and performed on MATLAB/SIMULINK. The controller and observer was implemented with a Matlab function block, where the digitization is considered. To proof the stability of the system and the compensation of the gyroscopic effect, Fig. 8 shows a Campbell diagram of the system, which is controlled with the presented control structure. The natural frequencies are time invariant and there is only one resonance for the translation and one for the tilting movement. This proves the independence of the angular velocity of the compensated system. Compared to Fig. 3 this simulation result shows stability for the whole speed range.

The second simulation deals with sensitivity functions, which are a measure for the robustness of the system. According to ISO 14839-3 the peak value of the sensitivity function should be below 3. Fig. 9 and Fig. 10 shows the sensitivity of the tilting and the translation movement at operating speed, where the peaks of both functions are below a factor of 3. The peaks of this function are the least distances to the Nyquist point. From this fact can be stated, that the AMB system is robust against a variation of the dynamic parameters.

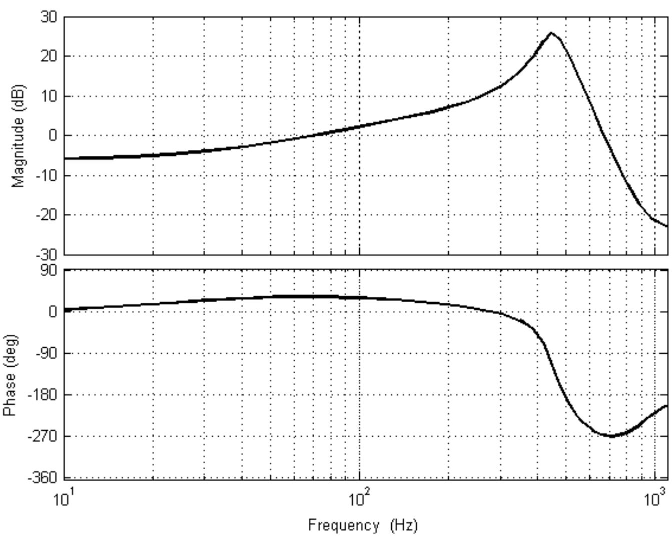

Fig. 7. Simulated transfer function of the tilting controller

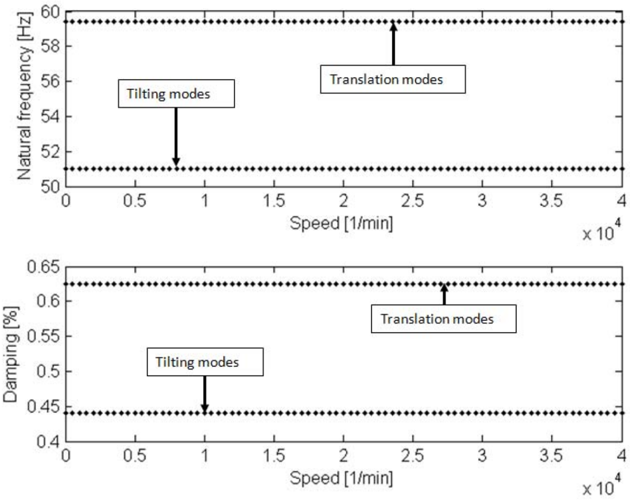

Fig. 8. Simulated Campbell diagram with the presented control structure

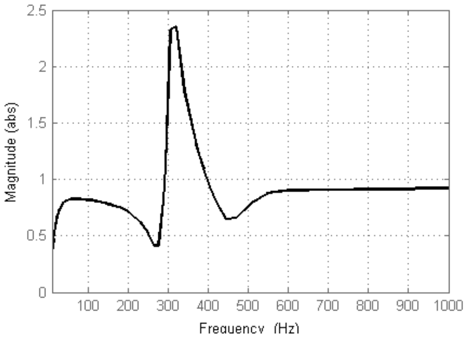

Fig. 9. Simulated sensitivity function of the tilting movement

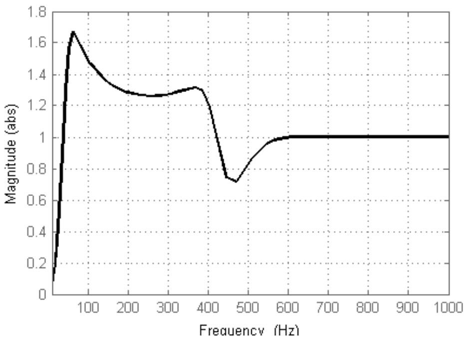

Fig. 10. Simulated sensitivity function of the translation movement

V. Experimental results

The aim of this section is to verify the velocity independence and the robustness of the system, according the simulations in the previous section. In the following subsections the measured sensitivity functions of the tilting and the translation movement and a comparison of the dynamic behaviour from the system at standstill and at operating speed are presented.

A. Sensitivity functions at operating speed

In this subsection the measured sensitivity functions of the tilting and translation movements are discussed and compared

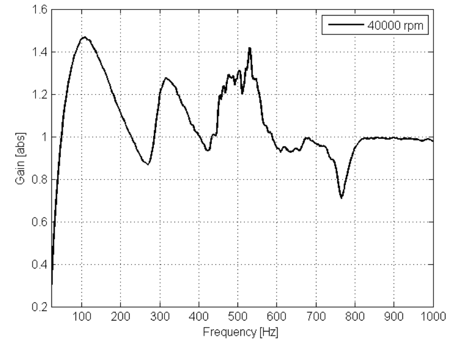

Fig. 11. Measured sensitivity function of the tilting movement

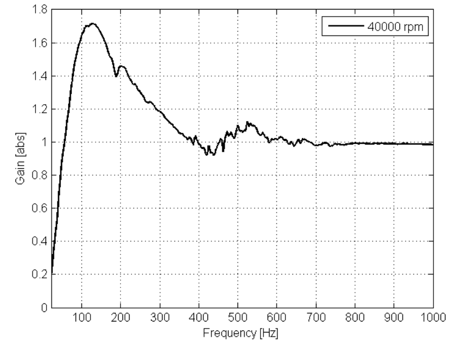

Fig. 12. Measured sensitivity function of the translation movement

to the results of the simulations. Fig. 11 and Fig. 12 shows that the measured sensitivity functions compared to the simulated sensitivity functions from Fig. 9 and Fig. 10 have nearly the same shape. The biggest difference is at the first and the second peak of the tilting movements. This differing shape is caused by a different behaviour of the rigid body modes of the simulated and measured model. The second peak of the tilting movement depends on the dynamic of the Kalman observer and C_{att}. If the compensation would be ideal, this second peak would not occur. In summary, the robustness of the system is proved, because the maximum values of the sensitvity functions are below three.

B. System behaviour at standstill and at high rotational speed

To verify, if the rigid body modes are time invariant in the real system, the dynamic behaviour at standstill and operating speed, were compared. For comparison the compliance transfer functions of the tilting and translation movement were used. Due to the symmetry of the dynamic behaviour in the x and y direction, only one tilting and one translation transfer function is necessary. Fig. 13 shows the comparison of the tilting compliance functions. The gain of both transfer function differs slightly. The reason is a not modelled effect, caused by the AMB application. The phase shows that the rigid body modes of the tilting movements are nearly the same for both operating speeds and the natural frequencies are at about 60Hz. The resonances at 200Hz at standstill and 300Hz with operating speed can also be measured in the open loop transfer function. This is an indication for a vibration caused by the control plant, which is not modelled. The natural frequency of the first

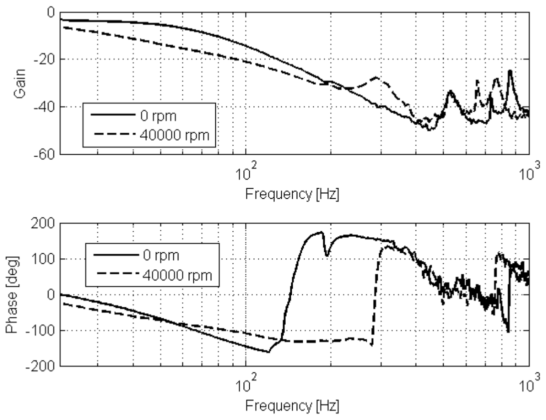

Fig. 13. Measured compliance function of the tilting movement

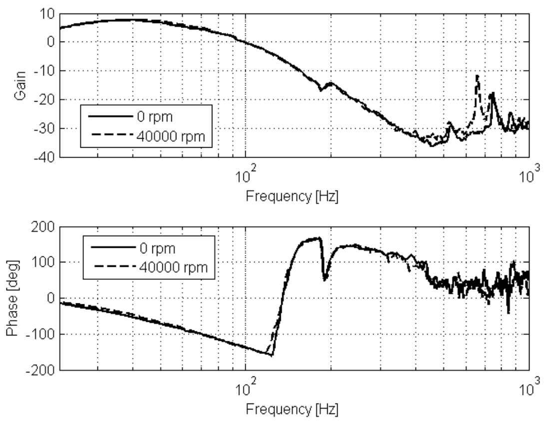

Fig. 14. Measured compliance function of the translation movement

bending mode at standstill is at about 860Hz and splits up for operating speed into one bending mode with a backward whirl at about 780Hz and one with a forward whirl which cannot be seen in this transfer function. In this paper only the gyroscopic effect of the rigid body modes is compensated, because all the other effects do not show stability problems. In contrast to this the rigid body modes without this compensation will have stability problems according to Fig. 3.

Fig. 14 shows the comparison of the translation compliance functions. Both transfer functions are nearly equal. This fact proves the functionality of the transformation in the COG coordinate system. From the phase plot can be seen that the natural frequency of the translation rigid body modes are at about 60Hz. The phase plot do not show a phase step due to the first bending mode. The reason is that the first bending mode is not well observable for translation movements with this rotor. In summary, can be stated that the designed decoupled controller fullfills the requirements for a stable and robust system.

VI. Conclusion

In this paper a decoupled control and a special parameter variant structure for a high gyroscopic rotor were designed. The resulting system of the combination of these two structures is a nearly linear parameter invariant system, only for the rigid body modes, for a high angular velocity range. It is verified that the natural frequencies of the rigid body modes of the AMB system are nearly the same for all angular velocities up to full speed. For control design the system was split up into a tilting and a translation part using a coordinate transformation. The functionality of this transformation was proved by experiments. To estimate the states for the compensation a Kalman filter was designed in the COG coordinate system. This coordinate system has the advantage, that the Kalman observer splits up into one observer for the tilting and one for the translation movement. This fact reduces the computing time of the observer significantly. To stabilize the first bending modes a lead lag filter in combination with a second order low pass filter was used. In summary can be stated, that for a high gyroscopic rotor the presented control structure, is a good choice for a stable system up to very high speeds. The main advantage of the presented method is that the reason of instability, caused by the gyroscopic effect, is eliminated. In contrast to this the state of the art controls usually permits the split up of the tilting rigid body modes. For such a system the controller needs to be very robust and cannot be optimal for both tilting modes, compared to the presented method.

Acknowledgment

This work is conducted within the project P21631-N22 of the Vienna University of Technology with the Austrian Science Fund (FWF). The authors thank the Austrian Science Fund for supporting this project.

References

[1] R. D. Williams, F.J. Keith, and P.E. Allaire, *Digital Control of Active Magnetic Bearing*, IEEE trans. on Indus. Electr, February 1990.

[2] H. Bleuler, C. Gähler, R. Herzog, R. Larsonneur, T. Mizuno, R. Siegwart, *Application of Digital Signal Processors for Industrial Magnetic Bearings*, IEEE trans. on Control System Technology, December 1994.

[3] M. Hofer, *Design and Sensorless Position Control of a Permanent Magnet Biased Radial Active Magnetic Bearing*, PhD thesis, TU Vienna, 2013.

[4] M. Hofer, E. Schmidt and M. Schrödl, *Design of a Three Phase Permanent Magnet Biased Radial Active Magnetic Bearing Regarding a Position Sensorless Control*, IEEE, 2009.

[5] H. Bleuler, *Decentralized Control of Magnetic Rotor Bearing Systems*, PhD thesis, Federal Institute of Technology Zürich, 1984.

[6] M. Ahrens and L. Kucera, *Cross feedback control of a magnetic bearing system*, Proceedings of the Third International Symposium on Magnetic Bearings, Federal Institute of Technology Zürich.

[7] G. Schweitzer, *Magnetic Bearings Theory, Design, and Applications to Rotating Machinery*, Springer Berlin, 2009, ISBN: 978-3-642-00496-4.

[8] M. Hutterer, M. Hofer, T. Nenning and M. Schrödl, *LQG Control of an Active Magnetic Bearing with a Special Method to consider the Gyroscopic Effect*, 14th International Symposium on Magnetics Bearings, Linz, 2014.

[9] J. Schmied and A. Kosenkov, *Practical controller design for rotors on magnetic bearings by means of an efficient simulation tool*, 10th International Conference on Vibrations in Rotating Machines, 2000.

[10] R. Herzog, P. Bühler,, C. Gähler and R. Larsonneur, *Unbalance Compensation Using Generalized Notch Filters in the Multivariable Feedback of Magnetic Bearings*, IEEE Transactions on Control Systems Technology, September 1996.

[11] K. J Aström, *Computer Controlled Systems Theory and Design*, Prentice Hall Information and System Sciences Series, 1997, ISBN-13: 978-0133148992